Preparation and Characterization of Urea/Formaldehyde/*Rosa Canina sp.* Seeds Composites

A. Gürses[a,*], S. Karagöz[a], F. Mindivan[a], K. Güneş[a], Ç. Doğar[b] and S. Aktürk[c]

[a]Faculty of K.K. Education, Department of Chemistry, Atatürk University, 25240, Erzurum, Turkey
[b]Faculty of Education, Department of Science, Erzincan University, 24030, Erzincan, Turkey
[c]Faculty of Science, Department of Physics, Muğla University, 48000, Muğla, Turkey

Urea–formaldehyde (UF) resin which is one of the most important wood adhesives is a polymeric condensation product of the chemical reaction of formaldehyde with urea, and considered as the most important type of adhesive resins for the production of particleboards. The present study is aimed to preparation and characterization of urea/formaldehyde/*Rosa Canina sp.* seeds — and urea/formaldehyde/*Rosa Canina sp.* seeds/organo clay composites and also to determine the utility as an alternative and low cost material to manufacture particleboard. The synthesis of various composites was carried out using fresh *Rosa Canina sp.* seeds, typical agricultural waste, in its changing ratios from 7.7 to 83.3 wt%. Also, some of the composite mixtures were prepared by adding organo clay (0.17–3.3 wt%) in a constant ratio of 1/1 wt of urea and formaldehyde. The structural and mechanical characterization of samples was performed by X-ray diffraction, Fourier transform infrared spectra, high resolution transmission electron microscopy images and measurements of Shore D and scratch hardness. The analysis results conclude that organo clay platelets dispersed as simultaneously intercalated and exfoliated in resin matrix and also the increased organo clay ratio led to increase in the hardness values of samples.

1. Introduction

Urea–formaldehyde (UF) resin adhesive is a polymeric condensation product of the chemical reaction of formaldehyde with urea, and considered as one of the most important wood adhesives among melamine–urea–formaldehyde (MUF) resins, melamine–formaldehyde (MF) resins and phenol–formaldehyde (PF) resins [1–3]. Urea formaldehyde resins have been greatly used in the production of particleboard and other wood based panel industries. The use of urea formaldehyde resin as a major adhesive by the forest products industry is due to low cost, low cure temperature, water solubility, lack of color and ease of use under a wide variety of curing conditions [4]. UF resin adhesives also possess a critical disadvantage, formaldehyde emission from the panels. The formaldehyde content of UF resins has been gradually lowered over the years because it is one of the most effective ways of reducing formaldehyde emission. The emission of formaldehyde decreases as the mole ratio falls, but unfortunately, the other physical and mechanical properties were influenced negatively at the same time [5]. In this study, the mechanical properties of prepared composites at the lower formaldehyde ratios has been tried to be improved by the addition the given quantities of organoclay to UF resin/*Rosa Canina sp.* seeds mixtures.

The past 40 years have seen the successful developments within the forest products industry especially in products generally referred to as particleboards. Much of this success can be attributed to the decided economic advantage of low cost wood raw material and inexpensive processing with binders. Construction and furniture industries are the largest markets for the board. Particleboards have found applications in floor, wall, and ceiling panels, office dividers, bulletin boards, furniture, cabinets, counter tops, and desk tops. Agricultural residues are the renewable resources that can be utilized as raw materials for particleboard manufacturing [6]. Among the raw materials are pumice, kiwi prunings, wheat straws, bamboo, cotton seed hulls, flax shiv, rice straw-wood, vine prunings, coir pith, groundnut shells, waste of tea leaves, bagasse, cotton, hemp and jute stalks, sunflower stalks, maize husk and cab, and wood floor. Urea–formaldehyde, phenol–formaldehyde, polyethylene and polyvinylidene are extensively used as a binder [1]. Among these binders, urea–formaldehyde is the most economic and useful glue because of its low cost and easy production [7]. The present study aim is preparation and characterization of urea/formaldehyde/*Rosa Canina sp.* seeds and urea/formaldehyde/*Rosa Canina sp.* seeds/organoclay composites.

2. Experimental

2.1. Materials

Urea, formaldehyde aqueous solution (37 wt%) and sulfuric acid (98 wt%) for synthesis were supplied from Merck. *Rosa Canina sp.* seeds were used as the raw material from Gümüşsu Herbal Tea Plant wastes, Gümüşhane, in Turkey. Proximate and ultimate analysis results of *Rosa Canina sp.* seeds are given in Table I. Some physical properties of the raw clay which has been taken from Erzurum, Turkey are given in Table II.

*corresponding author; e-mail: ahmetgu@yahoo.com

Chemical and mineralogical compositions of the raw clay are shown in Table III. The cation exchange capacity (CEC) of clay was determined by the ammonium acetate method [8]. The cetyltrimethylammonium bromide (CTAB) used as modifier was purchased from Merck and it was used without further purification.

TABLE I

Proximate and ultimate analyses of *Rosa Canina* seeds.

Component	[%]	Element	[wt%]
moisture	5.50	C	41.36
ash	2.79	H	6.03
volatile matter	66.34	N	1.20
fixed carbon	25.37	S	0.10
		O	51.31

TABLE II

Some physical properties of raw clay.

clay content [%]	76.00
cation-exchange capacity [meq/100 g dry soil]	48.90
specific gravity [g/cm^3]	2.61
organic matter content [%]	5.10
liquid limit, wL [%]	102.00
plastic limit, wP [%]	35.00
plasticity index, Ip (wL–wP)	67.00
BET (N$_2$) surface area [m^2/g]	64.20

TABLE III

Chemical and mineralogical compositions of raw clay.

Components	[%]	Mineral	[%]
SiO$_2$	56.77	smectite	25.84
Al$_2$O$_3$	15.66	chloride	19.76
MgO	8.79	illite	16.72
CaO	8.44	kaolinite	13.68
K$_2$O	4.04	analcime	11.00
Na$_2$O	4.20	calcite	7.00
SO$_3$	0.91	quartz	3.00
TiO$_2$	0.84	feldspar	3.00
P$_2$O$_5$	0.37		

2.2. Preparation of UF composites

2.2.1. Organoclay synthesis

In order to control interactions between the resin matrix and clay particles, it is necessary to expand the basal distance between clay layers and to make organophilic by using a modifier as CTAB. After 5.0 g of raw clay was dispersed in a shaker containing 2.5 L distilled water, the mixture was shaken in order to swell it at 150 rpm for 30 min and then concentration of the clay/water suspension was adjusted as 160 mg/L in CTAB and continued to shaking for 1 h. Finally, the mixture was filtered, washed, and dried for 1 h at 110 °C under a vacuum and milled.

2.2.2. Preparation of UF/Rosa Canina sp. seed and UF/Rosa Canina sp. seed/organoclay composites

The experimental setup for the urea–formaldehyde reaction consists of a glass reactor equipped with a mechanical stirrer, a thermometer, and a reflux condenser. The synthesis of composites in the various compositions (see Table IV) was carried out using dried *Rosa Canina sp.* seeds, typical agricultural waste, in its changing ratios from 7.7 to 83.3 wt% at 60–70 °C. The prepared urea/formaldehyde/*Rosa Canina sp.* seeds composites are coded as UF2–11.

TABLE IV

The combinations of UF/*Rosa canina sp.*/organoclay composites.

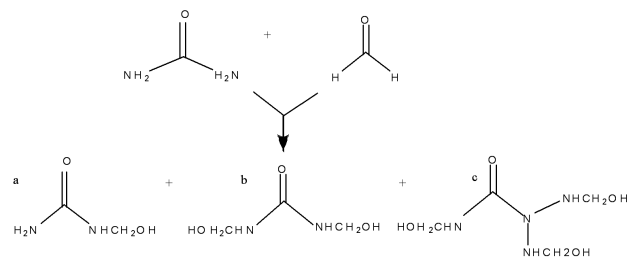| UF composites	U/F (urea/ formaldehyde) [wt]	*Rosa canina sp.* [wt%]	Organo-clay [wt%]
UF1	3/3	–	–
UF2	3/3	7.7	–
UF3	2.5/2.5	16.6	–
UF4	2.25/2.25	29.0	–
UF5	2.0/2.0	33.3	–
UF6	1.75/1.75	41.6	–
UF7	1.5/1.5	50.0	–
UF8	1.25/1.25	58.3	–
UF9	1.0/1.0	66.6	–
UF10	0.75/0.75	75.0	–
UF11	0.5/0.5	83.3	–
UF12	–	100.0	–
UF13	1/1	66.5	0.17
UF14	1/1	66.1	0.50
UF15	1/1	65.8	0.80
UF16	1/1	65.0	1.60
UF17	1/1	64.1	2.50
UF18	1/1	63.3	3.30

Fig. 1. Formation of (a) mono-, (b) di-, and (c) trimethylolurea by the addition of formaldehyde to urea.

Also, some composites were prepared by adding organo-clay (0.17–3.3 wt%) in a constant ratio of 1/1 wt of urea and formaldehyde with changing ratios of *Rosa Canina sp.* seeds and the composites containing organoclay are coded as UF13–18. At the end of each synthesis, the mixture followed by adding a few drops concentrated sulfuric acid was pelleted at pressure of 6.0 tone/cm^2 and 70 °C. UF resins are thermosetting
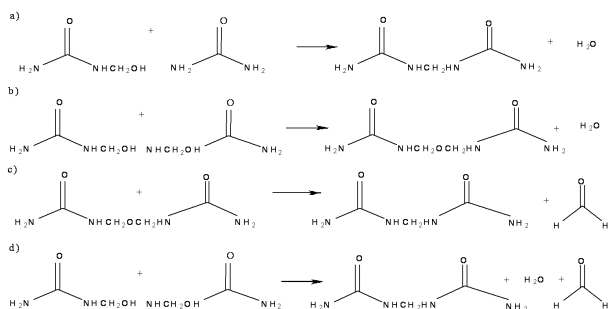
Fig. 2. Condensation reactions of methylolureas to form (a) methylene bridges between amido nitrogens, (b) methylene ether linkages and (c), (d) methylene linkages.
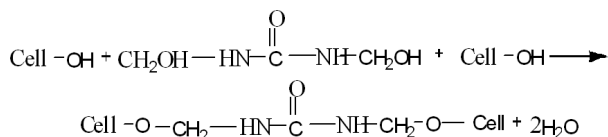

Fig. 3. The proposed reaction for methylolureas and cellulose molecules.

polymers, prepared by the reaction of two monomers, urea and formaldehyde. This reaction is basically a two--step process: usually an alkaline methylolation followed by an acid condensation. Methylolation refers to the addition of up to three molecules of the bifunctional formaldehyde to one molecule of urea to give the so-called methyloureas (Fig. 1). This reaction presents a series of reactions that lead to the formation of mono-, di- and trimethylolureas. Degradation process of cured resin begins with liberation of formaldehyde from dimethylene ether groups (Fig. 2) [9].

Also, the proposed reaction between methylolureas and cellulose molecules is given in Fig. 3 [10].

2.3. Characterization of UF composites

Many techniques, such as X-ray diffraction (XRD), Fourier transform infrared (FTIR), and high resolution transmission electron microscopy (HRTEM), have been incorporated to characterize the composites in this study. XRD diffractograms for the composites and filler materials were taken in Bruker D8 Advance X-ray Diffractometer with a Cu K_{α_1} (1.540 Å) radiation, operating at 40 kV and 30 mA over a 2θ range of 1.5–40°. The scanning rate of the instrument was 2°/min. FTIR spectra for the commercial organoclay, colored organoclay and prepared composites were taken on a Perkin-Elmer Spectrum-One, by KBr pelleting method from 4000 to 400 cm^{-1}. All measurements were obtained by an average of 100 scans and a resolution of 1 cm^{-1}. The specimens from the samples were examined by using a JEOL 2100 high resolution transmission electron microscope (LaB$_6$ filament) operated at 200 kV.

2.4. Mechanical analysis

2.4.1. Scratch tests

Scratch tests were performed by rubbing Rockwell C diamond indenter on the coatings under a constant normal load of 5 N with a speed of 0.007 m/s.

The scratch hardness was computed using the following equation [11]:

$$H_s = q\frac{4W}{\pi d^2},$$

where W is the normal load (N), d is the recovered scratch width (m), and q is a coefficient which is a function of the elastic/plastic behavior of the softer material ($q = 1$ for very elastic contact without fracture and $q = 2$ when there is high amount of plastic deformation). Here, we assumed q equal to 1.5 as the purpose of this study was to compare the scratching performance of the UF composites and hence a fixed value of q would suffice.

2.4.2. Shore D tests

Shore hardness is a measure of the resistance of a material to the penetration of a needle under a defined spring force. It is determined as a number from 0 to 100 on the scales A or D. The higher the numbers, the higher the hardness. The letter A is used for flexible types and the letter D for rigid types. Measurements were performed at room temperature. Shore D hardness scale was used and the average of 10 hardness values was taken.

3. Results and discussion

3.1. FTIR analysis

All the resins were pretreated under the same conditions. Figure 4 represents the important characteristic bands for virgin UF resins. The FTIR spectrum of *Rosa Canina sp.* seed is seen in Fig. 4.
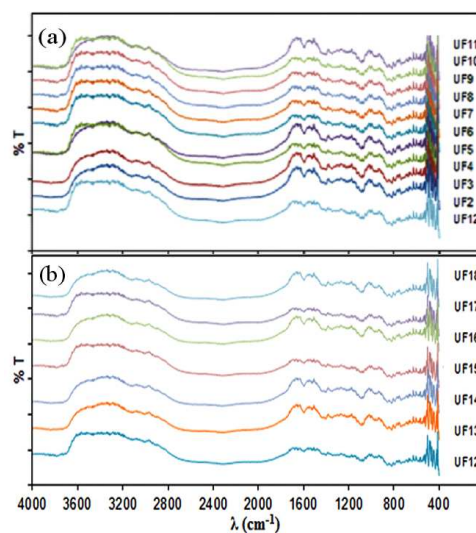

Fig. 4. FTIR spectra for *Rosa Canina sp.* seeds reinforced UF composites (a) and *Rosa Canina sp.* seed and organoclay reinforced UF composites (b).

As shown in Fig. 5a, the peaks at 1555 cm^{-1} began to appear to NH-bending vibration (NH-CO), not seen

in pure cellulose and the signals decreased with increase of the amount of cellulose then the composite of UF6, except UF11. The band at 1669 cm^{-1} was not assigned to the stretching C=O vibration in –CONH$_2$. This situation does not show the structure of the free urea.

C–O vibration of ether appeared at 1024 cm^{-1} and polymerization does not affect these vibrations. This type of connecting reveals that there is an attachment from the hydroxyl groups once again. The peak is observed unaffected from polymerization at 2965 cm^{-1} and is attributed to the CH mode of CH$_2$ of ether and CH$_2$OH

and N–CH$_2$. The sharp peak at 1650–1630 cm^{-1} corresponds to N–H bending vibrations at UF2, UF3, UF5, and UF11. The amount of cellulose can be attributed to the interaction between hydroxy groups with the amino group except UF5 and UF11. In the rate of too high cellulosic material it is observed that the intensity of the peak increased. The band at 3500 cm^{-1} was not assigned to N–H vibrations of primer amine at the composites of UF5 and UF11. So methyl bridges are established and consist of a more compact construction in these composites.
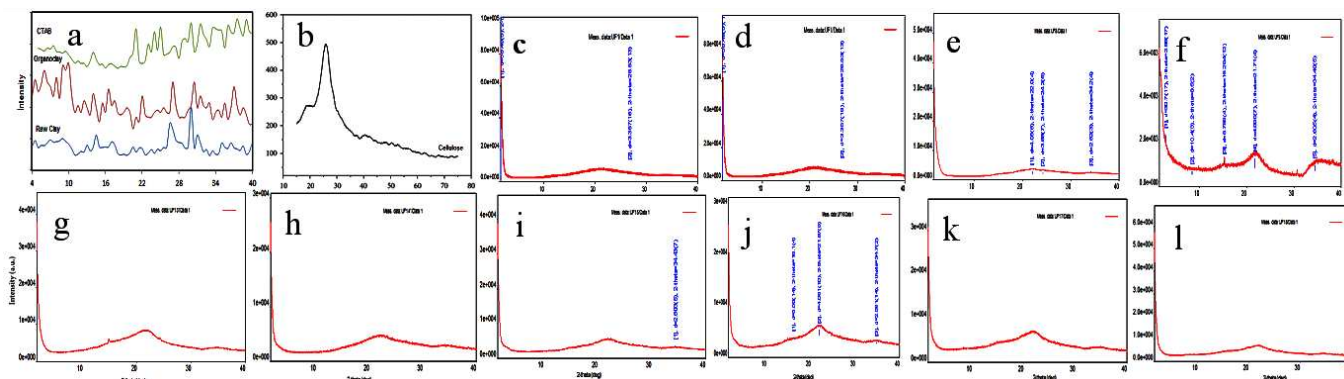

Fig. 5. XRD diffractograms for the raw clay, the synthesized organoclay and CTAB (a) and the cellulose as a prototype to *Rosa Canina sp.* seeds (b), UF (c), *Rosa Canina sp.* seeds reinforced composites UF6 (d), UF8 (e), UF9 (f); *Rosa Canina sp.* seeds and organoclay reinforced composites UF13 (g), UF14 (h), UF15 (i), UF16 (j), UF17 (k), UF18 (l).

The range 1150–1100 cm^{-1} is associated with bending and stretching vibration of C–O and ether vibrations of C–O–C. This shows that there are both the cellulosic material and smaller oligomeric structures in the matrix. The peak at 1540 cm^{-1} does not appear to bending peak –NH at UF2, UF3, UF5, and UF11, because they are widely composed of methylene bridges. The peak at 909–666 cm^{-1} was observed to be due to vibration of –NH peaks in pure and all other composites. As can be seen in Fig. 5b, NH-bending vibration appears at 1555 cm^{-1} at UF13, UF14, and UF16 and UF18, which are related to *Rosa Canina sp.* seeds and organoclay reinforced composites. The peak at 2965 cm^{-1} is attributed to the CH mode of CH$_2$ of ether and CH$_2$OH and N–CH$_2$. The peaks for UF13, UF14, and UF16 indicate the formed trimethylol bridges. The composites of UF15, UF17, and UF18 have peaks showing polymerization, which occurs with mono- and di-methylol bridges (probably with the interactions between the polymer and cellulose).

3.2. XRD analysis

Wide angle X-ray analysis (XRD) was carried out to investigate the effectiveness of the clay intercalation or exfoliation and if any change in crystalline structure of the UF resin occurred [12]. Figure 5 shows the results of X-ray diffractograms of the raw clay, organoclay, CTAB, and UF composites depending on the *Rosa Canina sp.* seeds and organoclay different ratios, respectively. XRD

diffractograms for the raw clay, the synthesized organoclay and CTAB (Fig. 5a), and the typical cellulosic material (Fig. 5b) are given in Fig. 5.

As seen from this figure, the wide smectite peak for raw clay at 6–8° has shifted to left. This depicts that intercalation of CTA$^+$ ions from solution into the interlayer region of the clay has occurred and the CTA$^+$ ions adsorbed to the surface of clay platelets lead to a significance in the basal distance.

According to diffractogram of the organoclay, from Fig. 5, it can be seen that CTAB enters into interlayer region. The raw clay showed that wide smectite peaks were at a range of 6–8°. The peak of organoclay has partly shifted to left. This implies to an expansion in the basal distance in consequence of intercalation of CTA$^+$ ions.

In Fig. 5c, virgin UF resin showed highly crystalline behavior at an angle of 15–22°. From Fig. 5d–f, it can be seen that the main polymer peak was sharpened with increase of the amount of *Rosa Canina sp.* seeds. It was observed that the addition of these seeds caused a positive effect on crystallization and especially at the higher ratio of seeds; different crystalline structures emerged such as derivatives of mono-, di-, and trimethylolurea. UF resins at lower F/U mole ratio from 1.1 to 0.5 show crystal structure while UF resins with higher F/U mole ratio are amorphous polymers [3]. Although the mole ratio

of F/U in this study is taken as 1.0, after adding organoclay to the resins, their crystalline structures deforms due to formation of exfoliated-intercalated structures in polymeric matrix (Fig. 5d and e).

Figures 5g and h depict that a broad doublet peak occurs due to overlapping peaks for virgin UF (Fig. 5c) and cellulosic material at 25°–39° (Fig. 5b). When the organoclay is almost completely dispersed, the peak for it does not appear [13]. In the higher ratios of organoclay such as at UF15 the intensity of polymer peak decrease and smaller peaks disappears as parallel to decrease of the amount of cellulosic material compared with the above-mentioned composites. This decrease in signal intensity is probably due to the deformation of the crystal structure of cellulosic material. For this composite it can be suggested the presence of mutual interactions between cellulosic fibers and the polymeric matrix [14]. The tertiary interactions between them might hinder with clay loading into the polymeric matrix.

XRD diffractograms for UF16 and UF17 show the peak for the polymer became clearer indicating a positive effect on crystallization of presence of organoclay. In the formation of crystal, especially it can be said that the mono-methylol derivatives for the polymer have a dominant effect on crystallization. The addition of excess organoclay to polymer matrix as parallel to the decrease in the amount of fibrous material may lead to the decreased cross-linking in the matrix and thus to decrease in the degree of crystallization [15].

3.3. HRTEM analysis

Although XRD is a very convenient way to investigate the interlayer spacing of silicate layers in the original state and in the intercalated nanocomposite, peak broadening, and intensity variation are difficult to be analyzed by it alone [16]. Also interpretation of spatial distribution or any structural non-homogeneity is limited with XRD. Therefore, XRD should be accompanied by TEM, which provides localized information on the hybrid structure [17]. It is important to note that TEM is only a qualitative technique, while XRD is a quantitative. Generally both techniques are used together concluding about the structures of nanocomposites [10]. In order to clarify the structures of UF composites, HRTEM micrographs for *Rosa Canina sp.* seeds and organoclay containing specimens were taken (Figs. 6 and 7). The virgin UF and UF composites which have low ratios of the seeds were compared with the other of HRTEM micrographs.
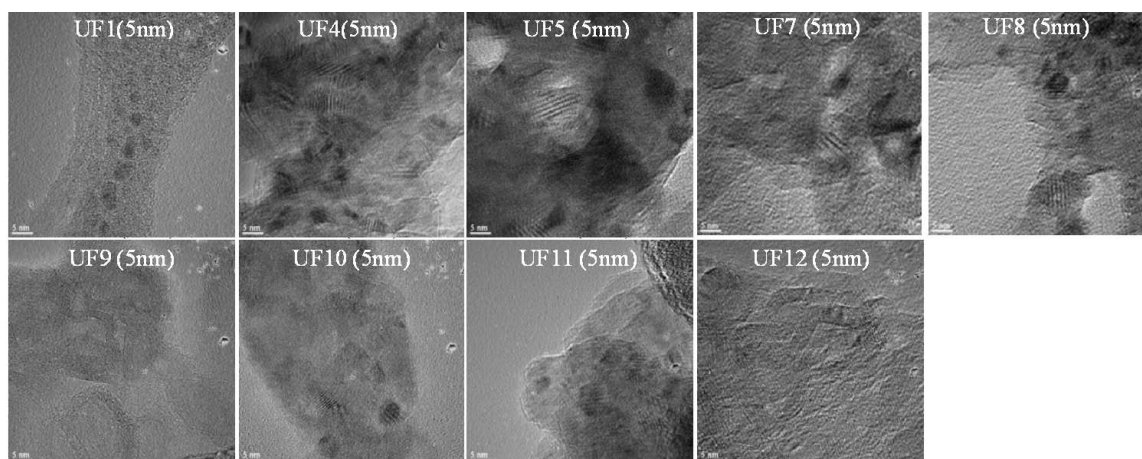

Fig. 6. HRTEM micrographs for UF composites containing *Rosa Canina sp.* seeds.
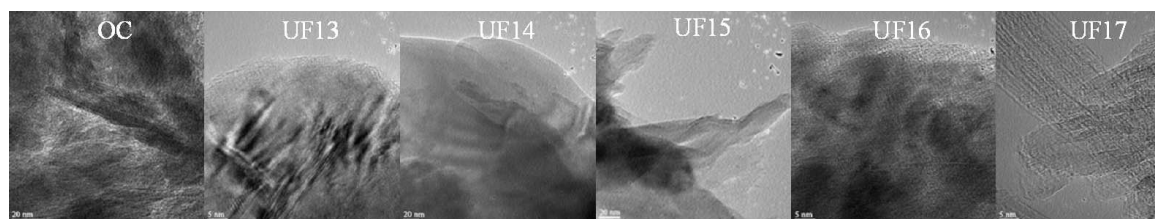

Fig. 7. HRTEM micrographs for *Rosa Canina sp.* seeds and organoclay containing UF composites.

From Fig. 6, it can be seen that the fibrous material completely dispersed the resin matrix. By increase in the amount of the seeds (UF4), the localized layered structures appeared, reflecting the interactions between the polymer chains and fibers. These structures appeared as more homogeneous ones in the case of UF5. It also was observed that the cross-linked and parallel interactions between the fibrous material and resin matrix occurred in the cases of UF7 and UF9. As can be seen from the micrographs for UF10 and UF11, the fibrous materials dis-

persed in the polymer matrix look like micro-crystalline or ordered blocks surrounded by polymer chains. From this figure, it can be seen that by increasing in the amount of the seeds the cellulosic fibers completely dispersed in the matrix. The HRTEM micrographs for virgin UF resin, fresh *Rosa Canina sp. Seeds*, organoclay and the composites are shown in Fig. 7, respectively.

From Fig. 7, it can be seen that the interaction between fibrous material and polymer chains is relatively homogeneous and the clay layers almost completely exfoliated.

3.4. Mechanical properties of the composites

In the samples which do not contain organoclay, except for UF11, UF4, and UF13 including the lowest amount of organoclay, hardness (Shore D) and scratch hardness values of the composites exhibit a similar trend with increased amount of cellulosic material. On the other hand, UF11, UF4, and also UF15 which contains a moderate amount of organoclay show a sharp increase in both hardness and scratch hardness. Therefore, it can be said that the presence of cellulosic material did not make a disturbing effect on the chain formation.
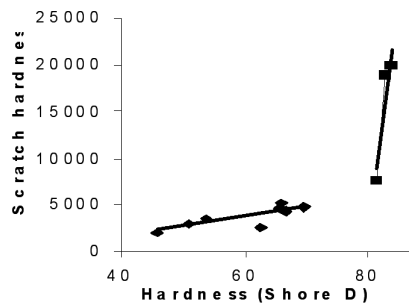
Fig. 8. Relationship between Scratch hardness and hardness (Shore D) for the composites.

Moreover, intensive interactions between the polymeric chains and the cellulosic material in the cases of UF4 and UF11 may have led to a high stable behavior. These interactions probably cause the formation of the cross linked polymeric chains and so the revealing of a compact matrix. UF15 exhibits a similar behavior, because organoclay plates in this composition may be taken on a positive role on the formation of polymeric chains.

4. Conclusions

- In this study, UF/*Rosa Canina sp.* seeds and UF/*Rosa Canina sp.* seeds/organo clay composites were prepared with *in situ* polymerization method.

- X-ray diffractograms depict that CTA^+ ions from bulk into the interlayer region of the clay intercalated and CTA^+ ions adsorbed onto the clay platelets lead to a significant increase in the basal distance.

- HRTEM images show that it can be seen that the fibrous material completely dispersed the resin ma-

trix. By increasing in the amount of the seeds, the localized layered structures appeared, reflecting the interactions between the polymer chains and fibers. These structures appeared as more homogeneous ones. It also was observed that the cross-linked and parallel interactions between the fibrous material and resin matrix occurred and the fibrous materials dispersed in the polymer matrix look like micro-crystalline or ordered blocks surrounded by polymer chains.

- Hardness (Shore D) and scratch hardness values of the composites with the low amount of organoclay exhibit a similar trend with increased amount of cellulosic material. The composites which contain a moderate amount of organoclay exhibit a sharp increase in both hardness and scratch hardness. Therefore, it can be said that the presence of cellulosic material did not make a disturbing effect at the formation of polymeric chains during the polymerization.

References

[1] M. Gürü, S. Tekeli, I. Bilici, *Mater. Des.* **27**, 1148 (2006).

[2] M. Dunky, *Int. J. Adhesion Adhesives* **18**, 95 (1998).

[3] B. Park, H. Jeong, *Int. J. Adhesion Adhesives* **31**, 524 (2011).

[4] K. Akyüz, G. Nemli, M. Baharoğlu, E. Zekovic, *Int. J. Adhesion Adhesives* **30**, 166 (2010).

[5] Z. Que, T. Furuno, S. Katoh, Y. Nishino, *Building Environment* **42**, 1257 (2007).

[6] D. Wang, X.S. Sun, *Ind. Crops Prod.* **15**, 47 (2002).

[7] G. Nemli, H. Kinrcin, B. Serdar, N. Ay, *Ind. Crops Products* **17**, 39 (2003).

[8] A. Gürses, M. Ejder-Korucu, C. Dogar, *Sci. World J.* **2012**, 270452 (2012).

[9] S. Samarzija-Jovanovic, V. Jovanovic, S. Konstantinovic, G. Markovic, M Marinović-Cincović, *J. Therm. Anal. Calorim.* **104**, 1159 (2011).

[10] G.E. Myers, *Proc. Wood Adhesives 1985*, Madison (WI) 1985, p. 119.

[11] S.K. Sinha, T.X. Song, W. Ytong., *Wear* **266**, 814 (2009).

[12] H. Lei, G. Du, A. Pizzi, A. Celzard, Q. Fang, *Wood Adhesives* **54**, 225 (2010).

[13] S.K. Gang, S.M. Lee, I.K. Sung, C.G. Kim, *Polymer Prep.* **51**, 1169 (2005).

[14] G. Rivero, A. Vázquez, L. Manfredi, *J. Appl. Polym. Sci.* **114**, 32 (2009).

[15] J. Pappas, K. Patel, E. Nauman, *J. Appl. Polym. Sci.* **95**, 1169 (2005).

[16] A.A. Sapalidis, F.K. Katsaros, Th.A. Steriotis, N.K. Kanellopoulos, S. Dante, T. Hauss, *J. Phys. Conf. Series* **2012**, 012090 (2012).

[17] M.H. Choi, I. Chung, J. Lee, *Materials* **12**, 2977 (2000).